Waste Isolation Pilot Plant

Compliance Certification Application

Reference 63

Berner, R.A. 1983.
Kinetics of Weathering and Diagenesis, Kinetics of Geochemical Processes. Eds. A.C. Lasaga, and R.J. Kirkpatrick. Min. Soc. Am. Reviews in Mineralogy Vol. 8, 111-133.

Submitted in accordance with 40 CFR §194.13, Submission of Reference Materials.

SENT BY:WIPP PURCHASING ; 11- 7-95 ; 3:19AM ; 0000000000000 ; 16105200763;# 3

DATE/TIME	LML STAFF	FILLED	UNFILLED

REGULAR FEDEX

LINDA HALL LIBRARY
OF SCIENCE, ENGINEERING AND TECHNOLOGY
5109 CHERRY STREET · KANSAS CITY · MISSOURI 64110-2498 USA
DOCUMENT SERVICES
1-800-662-1545 FAX 816-926-8785 ARIEL IP.198.209.22.122 EMAIL: REQUESTS@LMLINK.UMKC.EDU

Regular

3 HR SUPER RUSH FAX	8 HR RUSH FAX	24 HR FAX	FEDEX	ARIEL	1ST CLASS MAIL	BOOK LOAN	PICK UP	HAND COPY

Please ship by 11/20/95

PATRON'S COMPLETE ADDRESS

SHIPPING ADDRESS:
WESTINGHOUSE ELECTRIC - WASTE ISOLATION DIVISION
WIPP SITE
ATTENTION: MAIN WAREHOUSE
30 MILES SOUTHEAST OF CARLSBAD
CARLSBAD, NEW MEXICO 88220

BILLING ADDRESS: ATTN. ACCOUNTS PAYABLE P.O. BOX 2078
CARLSBAD, NEW MEXICO 88221

FAX (505) 885-8802
PHONE (505) 234-8880
FEDEX
DEPOSIT ACCOUNT # 10241
PURCHASE ORDER # 71788
MC VISA AMEX DISCOVER
#
USER EXP. DATE

AUTHORIZING SIGNATURE (FULL NAME) Mark Edwards Copyright Option

IMPORTANT! PLEASE INDICATE ONE OF THE FOLLOWING: CCL CCG CCC COPYRIGHT OPTION

JOURNAL, BOOK, CONFERENCE TITLE

Need 11 copies of the following:

AUTHOR

ARTICLE TITLE

Berner, R.A. 1983. "Kinetics of Weathering and Diagenesis," Kinetics of Geochemical Processes. Eds. A.C. Lasaga, and R.J. Kirkpatrick. Min. Soc. Am. Reviews in Mineralogy, Vol. 8, 111-133. 615/5 -00008

VOL / ISSUE DATE

CALL NUMBER / LOCATION PAGES 111-134 24

NOTICE:
WARNING CONCERNING COPYRIGHT RESTRICTIONS
THE COPYRIGHT LAW OF THE UNITED STATES (TITLE 17, UNITED STATES CODE) GOVERNS THE MAKING OF PHOTOCOPIES OR OTHER REPRODUCTIONS OF COPYRIGHTED MATERIALS. UNDER CERTAIN CONDITIONS SPECIFIED IN THE LAW, LIBRARIES AND ARCHIVES ARE AUTHORIZED TO FURNISH A PHOTOCOPY OR OTHER REPRODUCTION. ONE OF THESE SPECIFIED CONDITIONS IS THAT THE PHOTOCOPY OR REPRODUCTION IS NOT TO BE USED FOR ANY PURPOSE OTHER THAN PRIVATE STUDY, SCHOLARSHIP OR RESEARCH. IF A USER MAKES A REQUEST FOR, OR LATER USES, A PHOTOCOPY OR REPRODUCTION FOR PURPOSES IN EXCESS OF "FAIR USE," THAT USER MAY BE LIABLE FOR COPYRIGHT INFRINGEMENT. THIS INSTITUTION RESERVES THE RIGHT TO REFUSE TO ACCEPT A COPYING ORDER IF, IN ITS JUDGMENT, FULFILLMENT OF THE ORDER WOULD INVOLVE VIOLATION OF COPYRIGHT LAW.

2'd NOV 10 '95 10:53AM LINDA HALL LIBRARY

NOTICE: This material may be protected by Copyright law (Title 17, U.S. CODE)

Chapter 3

KINETICS of WEATHERING and DIAGENESIS

Robert A. Berner

INTRODUCTION

Most solid materials found near the surface of the earth are not thermodynamically stable there. Some outstanding examples are: unweathered igneous feldspars, semi-amorphous "clay" (instead of well-crystallized phyllosilicates), and fine-grained goethite (instead of hematite) in soils, and undecomposed organic matter, aragonite (instead of calcite), and opaline silica (instead of quartz) in marine sediments. This metastability arises from fundamental causes which are physical, biological, and chemical in origin. First, igneous and metamorphic minerals, stable only at elevated temperatures, are carried into the zone of weathering by such physical processes as uplift and volcanism, and the energy necessary for this to occur is derived from within the earth. Second, because of an input of solar energy and its trapping by photosynthesis, organisms are able to biologically synthesize organic matter and other unstable substances such as aragonite and opaline silica. Finally, during weathering and diagenesis less stable minerals can form because of chemical factors which bring about the inhibition of nucleation and growth of more stable phases.

The preponderance of metastability near the earth's surface is a direct consequence of the slowness of chemical reaction rates at low temperatures. Thus, kinetics plays more of a leading role in earth surface geochemistry than it does at higher temperatures. Furthermore, we can study the rates and mechanisms of reactions by observing various stages during reaction both in the field and in the laboratory. The purpose of this chapter is to show how several different aspects of chemical kinetics can be brought to bear on the study of two major earth surface processes: weathering and diagenesis. Before proceeding directly to discussions of weathering and diagenesis, it is necessary to present some fundamental kinetic concepts which will enable the reader to better understand the discussions.

SOME FUNDAMENTAL CONCEPTS

In this paper we will be mainly concerned with the crystallization and dissolution of minerals from aqueous solution and the bacterial decomposition of organic matter. Basic principles controlling these three processes are presented in this section. Discussion is based on the following references which may be consulted for further details: Nielsen (1964) and Ohara and Reid (1973) for crystallization, Berner (1978a) for dissolution, and Berner (1980) for all three processes.

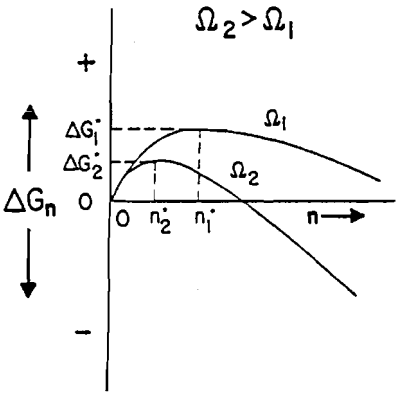

Figure 1. Plot of free energy of precipitation ΔG_n vs crystal size illustrating nucleation and growth. The free energy change increases up to a maximum due to nucleation and then decreases due to crystal growth. The diagram is for a single crystal containing n atoms, ions or molecules. Note the effect of the degree of supersaturation Ω on the position of each curve. (Modified after Nielsen, 1964 and Berner, 1980)

Crystallization

The crystallization, or precipitation, of a solid substance from aqueous solution can be divided into two processes: nucleation and crystal growth. Nucleation occurs prior to growth and distinction between the two processes can be made in terms of Figure 1. As a body precipitating from solution begins to increase in size (or in the number of atoms it includes) it encounters a free energy barrier to further growth. This barrier is a consequence of the fact that an interface between the growing body and the solution forms, and this results in an increase in free energy due to the creation of the interface. At small sizes the interfacial free energy dominates over the drop in free energy accompanying the relief of supersaturation, and as a result there is a net free energy increase. The free energy increases up to a maximum where the interfacial and bulk terms balance one another. At this point the body is referred to as the *critical nucleus* and the process leading up the free energy "hill" is called nucleation. During nucleation the body is referred to as a crystal embryo.

Once the critical nucleus has formed, further increase in its size can take place spontaneously with a net decrease in free energy.

This process is referred to as crystal growth and the growing body is considered a true *crystal*. Growth (and nucleation of other crystals) continues until enough material is removed from solution that supersaturation is relieved and equilibrium is attained.

As the degree of supersaturation is increased, the ease of nucleation is increased. This is shown in Figure 1 by a decrease in the size of the critical nucleus and a decrease in the free energy of nucleation, ΔG^* as the degree of supersaturation Ω is increased. (The parameter Ω is defined as the actual ion activity product divided by the equilibrium or solubility product.) The rate of nucleation is a strong exponential function of the free energy of nucleation; consequently, at high Ω values nucleation is very fast. Since nucleation and growth compete for dissolved material, at high degrees of supersaturation the rate of nucleation may be so fast that most of the excess solute is precipitated in the form of critical nuclei with little left over for growth. Since critical nuclei are commonly in the size range 10-100 Å, such rapid crystallization can result in the formation of a very fine grained precipitate. In this way the formation of poorly crystallized minerals in nature and in the laboratory can be explained. A common example is the reddish gelatinous precipitate of $Fe(OH)_3$ obtained by the mixing of concentrated solutions of ferric chloride and sodium hydroxide in the laboratory.

Low levels of supersaturation, by contrast, can result in good crystallinity. This comes about because the nucleation rate is so slow that most excess dissolved material is consumed by crystal growth on a limited number of critical nuclei. Most minerals which exhibit some degree of crystallinity from their x-ray diffraction patterns fall in this category. Thus, the rest of the discussion of crystallization will be devoted to crystal growth.

Crystal growth involves the transport of dissolved species to and from the surface of a crystal and various chemical reactions occurring at the surface. The latter includes adsorption, ion exchange, dehydration of ions, formation of two-dimensional nuclei on the surface, diffusion along the surface, ion pair formation, etc. The rate of growth is limited by the slowest step within a whole chain of processes and the nature of the rate-limiting step is not usually known. However, as a first approximation, the rate of crystal growth can be

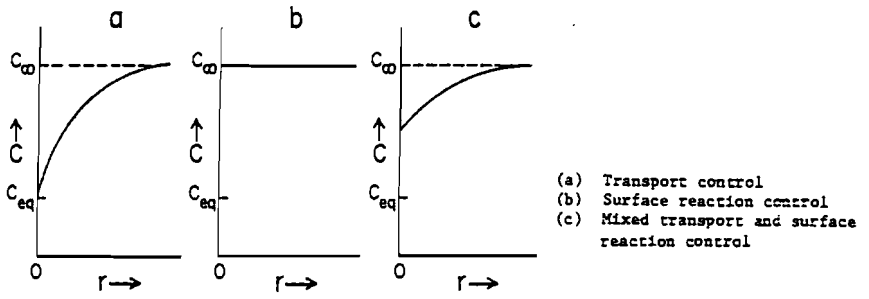

Figure 2. Schematic representation of concentration in solution C as a function of radial distance r, from the surface of a growing crystal. C_{eq} = saturation concentration, C_∞ = concentration out in solution. (After Berner, 1980)

characterized as being controlled either by transport of ions to the surface (transport-controlled), by reactions at the surface (surface-reaction controlled), or by a combination of both processes. A comparison of the three mechanisms is shown in Figure 2.

In pure transport-controlled growth (Fig. 2-a) ions (atoms, molecules) are added to the surface of the crystal so rapidly that migration of ions in solution to take their place cannot keep pace. As a result concentrations in solution adjacent to the crystal surface fall until they almost reach the equilibrium or saturation level. Further growth is limited by the rate at which additional ions can be transported to the crystal surface and the slowest process is that of molecular (ionic) diffusion. Transport to the surface can be accelerated by bulk flow of solution past the growing crystal or by stirring. Thus, transport-controlled growth is a strong function of the hydrodynamic state of the solution.

In pure surface-reaction controlled growth (Fig. 2-b) ion attachment to the surface is so slow that replenishment of ions in solution near the surface is easily accomplished by molecular diffusion and other transport processes. Concentrations in the near-surface zone are little different than those in the bulk solution, and growth rate is not affected by the hydrodynamic state of the solution.

Intermediate situations (Fig. 2-c) arise where ion attachment is sufficiently rapid that concentrations in the near-surface region are lower than they are in the bulk solution but not rapid enough to bring about a lowering to the saturation value. In this case the rate of growth is controlled by both transport and surface reactions.

Discernment of whether the rate of crystal growth of a given mineral is controlled by transport or surface-reaction can be accomplished by comparing measured rates of growth (from laboratory experiments or, preferably, from field methods) with those calculated for growth via molecular diffusion. Molecular diffusion is the slowest process by which crystals can grow and still have their rate controlled by transport. Faster measured rates indicate (advective) transport control whereas slower measured rates point to control by surface chemical reactions. Calculation of the approximate rate of growth via molecular diffusion is normally done using the expression (Nielsen, 1964):

$$\frac{dr_c}{dt} = \frac{\upsilon D_s (C_\infty - C_{eq})}{r_c} \qquad (1)$$

where: r_c = average radius of the crystals,
υ = molar volume of the crystalline substance,
D_s = coefficient of molecular diffusion in aqueous solution,
C_∞ = concentration in solution away from the crystal surface,
C_{eq} = equilibrium concentration adjacent to the crystal surface,
t = time.

For constant C_∞ (appropriate to an open system), equation (1) can be integrated to:

$$r_c = [2\upsilon D_s (C_\infty - C_{eq}) t]^{\frac{1}{2}} \qquad (2)$$

(Note that equations (1) and (2) are most correct when applied to equisized, equidimensional (*i.e.*, cubes, spheres, etc.) crystals separated by at least five diameters.)

Other ways of deducing overall growth mechanisms are through the use of different temperatures and different stirring rates in laboratory crystallization experiments. A stronger temperature dependence than that predicted for aqueous diffusion-controlled growth indicates a surface-reaction mechanism whereas a dependence on stirring rate, as discussed above, indicates transport control.

Actual mechanisms offered to explain surface-reaction controlled growth are varied and numerous. The two most commonly cited ones are surface nucleation control and dislocation control. In the former, rates of ion attachment are limited by the rate at which a new two-

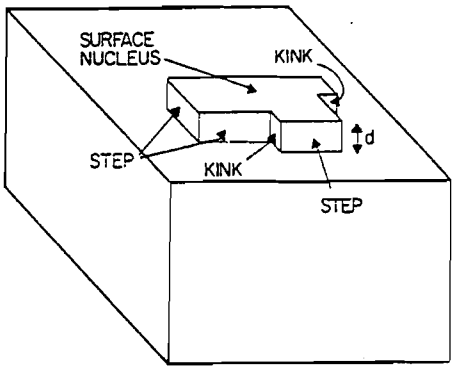

Figure 3. Idealized representation of the surface of a crystal. Dimension d represents one atom, molecule, unit cell, etc. On the flat crystal surface a "two-dimensional" surface nucleus is present which exhibits mon-atomic steps and kinks. (After Berner, 1980)

dimensional nucleus is formed on an otherwise atomically flat crystal face. The new nucleus is needed to provide unit-cell-sized steps and kinks on the surface which are energetically favored points of attachment. This is shown in Figure 3. In dislocation-controlled growth, built-in steps and kinks are provided by the intersection of screw dislocations with the crystal surface. By this mechanism the energy of surface nucleation is already provided by dislocation outcrops and growth spirals emanating from them, and, as a result, growth may occur at very low degrees of supersaturation. Although dislocation-controlled growth has been studied considerably, further discussion is beyond the scope of this paper, and the reader is referred to the book by Ohara and Reid (1973) or the classic work of Burton, Cabrera and Frank (1951) for additional details.

An important process, so far unmentioned, which can appreciably affect the rate of growth (and nucleation) of crystals from aqueous solution, is the adsorption of ions, molecules, etc., from solution onto the crystal surface (see Chapter 1). Natural waters contain many dissolved constituents which readily adsorb onto growing crystals, and some of these can serve as growth inhibitors. If normally available growth sites, such as kinks, are blocked by strongly adsorbed ions, then overall rates of growth can be greatly diminished. Also, preferential adsorption of such "poisons" onto certain crystal faces can result in the deceleration of their growth and a consequent alteration in crystal habit. Octahedral halite grown in the presence of urea is a classical example. The adsorption of inhibitors can so alter growth rates that normal rate dependences on supersaturation, as given for example by the usual models for dislocation-controlled growth (Burton *et al.*, 1951), are not obeyed (*e.g.*, see Ohara and Reid, 1973).

Dissolution

Like crystallization the overall process of dissolution of solids by an aqueous solution is controlled either by transport or by surface chemical reactions. The classification scheme shown in Figure 2 can also be applied to dissolution with the only difference being that concentrations adjacent to the crystal surface, for transport-controlled dissolution, are higher than they are in the bulk solution. Obvisouly, dissolution occurs only where undersaturation of the bulk solution is present, in other words, where $\Omega < 1$.

Methods for the discernment of the rate-controlling mechanism of dissolution are similar to those for crystallization. The rate of diffusion-controlled dissolution can also be obtained from equation (1). Note in this case that dr_c/dt is negative because C_{eq} is greater than C_∞. Comparison of measured rates of dissolution with that calculated for diffusion control, via equation (1), enables elucidation of the overall rate-controlling mechanism. Determination of the effects of temperature variation and stirring in the laboratory can also be used for the same purpose.

Dissolution is dissimilar to crystallization in one important respect. It is that three-dimensional nucleation is not necessary in dissolution since the dissolving crystals are already present. In fact, observations of partially-dissolved crystals can be used as an additional method for deducing the dissolution rate-controlling mechanism. In the case of rate control by surface reaction, slow partial dissolution of the surface results in the formation of crystallographically controlled features, such as large, well-developed etch pits. This arises from the fact that major dissolution originates only at points of excess energy on the surface such as dislocation outcrops. In the case of transport-controlled dissolution, attack of the surface is so rapid and non-specific that etching occurs virtually everywhere, and, as a consequence, only general rounding results. A comparison of morphological features produced by each mechanism for the same mineral, calcite, is shown in Figure 4.

As in the case of crystallization, rates of dissolution are considerably affected by the presence of adsorbed inhibitors. Such inhibition leads to surface-reaction controlled dissolution whose rate

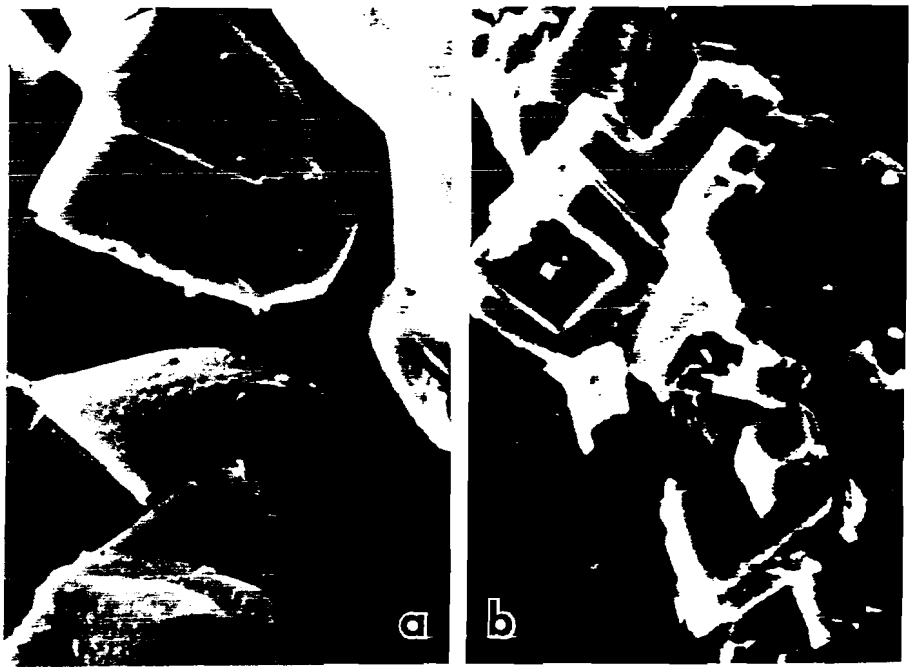

Figure 4. Electron photomicrographs of calcite which has undergone partial dissolution in seawater (X4000)

(a) Transport controlled dissolution; pH = 3.9. Note general rounding.
(b) Surface reaction controlled dissolution; pH = 6.0. Note angular, crystallographically controlled etch features.

(After Berner, 1978a, 1980 and Berner and Morse, 1974)

dependence on the degree of undersaturation is much greater than that predicted by commonly adopted theories. For example, the work of Morse (1978) and Keir (1980) has shown that calcite, under earth-surface conditions dissolves in seawater at a rate that is proportional to the fourth or fifth power of the concentration difference ($C_{eq}-C_{\infty}$). (Compare with equation (1).) This high-order kinetics is believed to be caused by the adsorption of dissolution-inhibiting phosphate ions onto the calcite surface (Berner and Morse, 1974; Morse and Berner, 1979).

Organic Matter Decomposition

Organic matter decomposition is discussed in the present paper because it exerts a major control on the chemistry and authigenic mineralogy of shallowly buried sediments. Rate laws for the decomposition of organic matter in sediments have not been well established. The model used here is that which I have used before (Berner, 1974; 1980). In it, it is assumed that the overall process of organic

decomposition (which includes a number of individual microbial steps) to CO_2 and other simple inorganic molecules, is first order with respect to the initial polymeric material undergoing decomposition. In other words:

$$\frac{dG}{dt} = -kG \qquad (3)$$

where: G = concentration of organic carbon undergoing decomposition (not total organic carbon),

k = first-order rate constant,

t = time.

The parameter G represents that fraction of the total organic matter actually undergoing decomposition at any given time. The reactivity, or k value, of organic compounds (*i.e.*, metabolizability) varies greatly and this is reflected by large variations in k from sediment to sediment and with depth in a single sediment (Toth and Lerman, 1977; Berner, 1978b; 1980; Jorgensen, 1978). Total organic carbon at the time of deposition is divided into various fractions, G_α, G_β, etc., according to their reactivity or k value. After deposition the most reactive compounds are destroyed first (G_α), followed by the next most reactive compounds (G_β), and so forth. As a result, sediments buried at slow rates contain only the less reactive organic compounds since the more reactive ones are destroyed at the sediment-water interface.

For each organic fraction designated as G the value of k varies with the process of decomposition. Organic matter in sediments is destroyed (microbially) by a variety of oxidizing agents in a definite succession (*e.g.*, Claypool and Kaplan, 1974). Dissolved oxygen is first used until it is entirely consumed, then dissolved nitrate until it is all gone, and then dissolved sulfate. Once all sulfate is used up there are no more inorganic oxidizing agents, and some of the organic carbon then appears as methane. Because of differences in free energy yields and metabolic pathways, decomposition of the same organic compounds by each of these processes can result in a different value of k in each case.

WEATHERING

The application of chemical kinetics to weathering is a relatively recent phenomenon. Most theoretical treatments of weathering have been in terms of equilibrium or irreversible, quasi-equilibrium models (Helgeson *et al.*, 1969; Fritz, 1975; Gac *et al.*, 1978; Tardy *et al.*, 1974; Fouillac *et al.*, 1977; Lindsay, 1979). One of the first workers to apply true chemical kinetics to weathering problems was Wollast (1967), who described the results of experiments in which ground K-feldspar was placed in buffered aqueous solutions and the release of silica with time was measured. Wollast found that the rate of addition of silica to solution decreased with time and he explained this decrease in terms of the formation of a protective layer of aluminous precipitate on the surface of the feldspar. The rate of dissolution was assumed to be controlled by the rate at which silica and cations could diffuse through the surface layer. Calculations based on a diffusion model, which is similar to that often used to describe the protective corrosion of metals, resulted in calculated diffusion coefficients D which are of the same order of magnitude as expected for solid diffusion (10^{-15} to 10^{-20} $cm^2 sec^{-1}$).

Subsequent workers (Helgeson, 1971; Pačes, 1973; Busenberg and Clemency, 1976) have expanded on the Wollast model and have suggested that the release of silica and cations from alkali feldspars can be described in terms of "parabolic kinetics" where the concentration in solution builds up in direct proportion to the square root of time. The protective surface layer is presumed to be either a precipitate of aluminum hydroxide and/or clay minerals, or "feldspar" in which the cations have been replaced by hydrogen (or hydronium) ions.

The concepts of parabolic kinetics and a protective surface layer formed on alkali feldspar during weathering have been tested by subsequent work (Petrović *et al.*, 1976; Petrović, 1976; Holdren and Berner, 1979; Berner and Holdren, 1979). In the studies of Petrović *et al.* and Holdren and Berner, ground sanidine and albite were subjected to leaching by aqueous solutions in the laboratory under conditions essentially identical to those employed by Wollast. Parabolic release of silica was found, but unexpectedly, the surfaces of the reacted feldspar grains were not found to be altered in any way. The Wollast model

predicts an altered surface of several hundred Ångströms thickness, but, using x-ray photoelectron spectroscopy (XPS), we found that no alteration product any thicker than about 5-15 Å could be present on the feldspar surface. In addition, we found that the parabolic kinetics could not be reproduced if the ground feldspar grains used for experimentation were first treated with HF to remove ultrafine and strained particles produced by grinding. This is shown in Figure 5. We obtained only linear kinetics, or a constant rate of release of silica to solution with time, with HF-treated material. We believe that the "parabolic" kinetics obtained by other workers is the result of varying rates of dissolution of particles produced during grinding. Very fine, submicron-sized particles, as well as strained regions on larger particles, because of excess surface free energy, should dissolve more rapidly than the larger grains. Initial silica release, therefore, should be faster due to preferential dissolution of the fine particles, and deceleration with time should occur as the particles are consumed. We actually observed disappearance of these particles during dissolution. From our results we conclude that feldspar dissolves in the laboratory according to linear kinetics and does not produce an altered surface layer. Parabolic kinetics is most likely an experimental artifact due to grinding.

Our laboratory results are esssentially verified from studies of feldspar grains taken from soils (Berner and Holdren, 1979). Under the scanning electron microscope (SEM) we found clay adhering to the surfaces of feldspar grains, but this clay could not have been protective in the sense envisioned by Wollast (1967). Shrinkage, upon drying (Fig. 6) shows that the clay is highly hydrous and not likely to be protective. (Typical diffusion coefficients in hydrous clay average about 10^{-6} cm^2sec^{-1}, not 10^{-15} to 10^{-20} cm^2sec^{-1} as required by the protective layer model.) Also, in most soils studied the clay does not adhere strongly (as would be expected if it were protective) since it can be removed by ultrasonic cleaning. Finally, examination of the surfaces of ultrasonically cleaned feldspar grains by XPS indicated a surface composition in the outermost few tens of Ångströms essentially identical to grain interiors. No cation depletion or aluminum enrichment, as expected for an altered surface layer, was found.

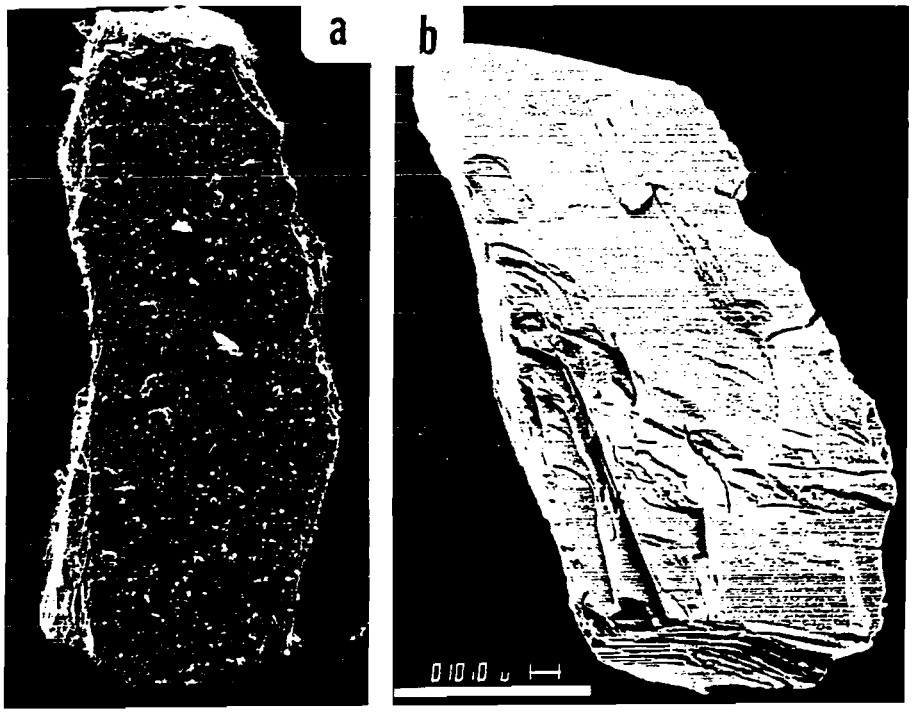

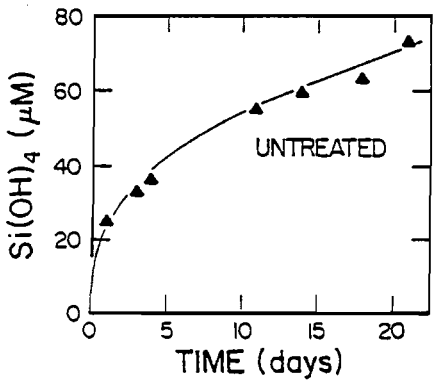

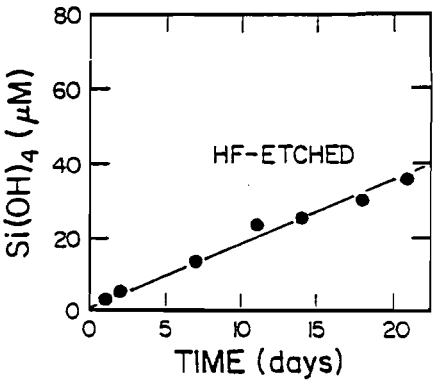

Figure 5. Effect of sample preparation on the dissolution behavior of albite feldspar. Albite grains, shown in SEM photomicrographs were (a) untreated and (b) HF-etched, after grinding. Each silica plot is for material pictured above it. (Adapted from Berner and Holdren, 1979)

Figure 6. SEM photomicrograph of a soil feldspar grain showing that clay adhering to the feldspar surface after ultrasonic cleaning has contracted and separated from the surface upon drying (see crack in center of photomicrograph). Sample from a gray-brown podzolic soil, Sangre de Cristo Mountains, New Mexico. (After Berner, 1978a and Berner and Holdren, 1979)

Figure 7. SEM photomicrograph of a feldspar grain (ultrasonically cleaned to remove clay) taken from a lateritic soil near Piedmont, N.C., U.S.A. Note prominent prismatic etch pits. (After Berner, 1978a; and Berner and Holdren, 1979)

If feldspar dissolution during weathering is not controlled by diffusion through a protective surface layer, then how does it dissolve? We feel, along with Aagaard and Helgeson (1981) and Dibble and Tiller (1981), that the limiting step in dissolution is not diffusion but chemical reaction at the feldspar-water interface. Proof of this is provided by SEM observations of ultrasonically cleaned feldspar grains taken from soils. The feldspar grains show the growth and development of characteristic, crystallographically-controlled etch pits on the surface which indicates dissolution rate control by surface chemical reaction (Wilson, 1975; Berner and Holdren, 1979). Some examples are shown in Figure 7. The etch pits indicate selective attack of the feldspar surface by soil acids, at points of excess energy such as dissolution outcrops. General attack of the surface with consequent rounding, as predicted for diffusion-controlled dissolution, is not found.

We discovered that we could duplicate the etch features found on soil grains by treating fresh feldspars with HF for extended periods in the laboratory (Berner and Holdren, 1979). Also, the same type of pitting (prismatic-shaped pits) was found on a variety of K and Na feldspars taken from several different soils where different soil acids should have been present. From this we conclude that pit shape is not sensitive to the type of acid attacking the feldspar as is the case for calcite dissolution (Keith and Gilman, 1960).

Our overall conclusions with regard to the dissolution of feldspar have been corroborated more recently from studies of pyroxene and amphibole dissolution, both in the laboratory and in soils (Berner *et al.*, 1980; Schott *et al.*, 1981). Pyroxenes and amphiboles also dissolve via linear and not parabolic kinetics in the laboratory when HF pretreatment is employed to remove ultrareactive fine particles produced by grinding. Dissolution in soils also produces characteristic etch pits showing that dissolution rate of pyroxenes and amphiboles is controlled by surface chemical reactions (example in Figure 8). One difference is that pyroxenes show some cation depletion, relative to silicon, on their surfaces, but this depletion extends to a depth of only a few Ångströms. This is too thin to be described as a diffusion-inhibiting protective surface layer. Diffusion loses all meaning when the total distance of diffusion is of the same order of magnitude as the size of the diffusing entities.

The mechanism of dissolution of minerals other than feldspars, pyroxenes and amphiboles during weathering has not been determined. Nevertheless, some prediction can be made. This is because there appears to be a reasonably good correlation between the solubility of a mineral and the rate-controlling mechanism by which it dissolves. This is shown in Table 1. The less soluble minerals all dissolve by surface reaction control. AgCl is an apparent exception but this may be caused by photochemical changes during kinetic studies, *e.g.*, see Nielsen and Söhnel (1971). Since most minerals involved in weathering have solubilities falling in the lower range shown in the table, it is likely that the rate of dissolution of many other minerals during weathering is also controlled by surface chemical processes and not by diffusion, either in aqueous solution or through protective surface layers.

Figure 8. SEM photomicrograph of a hornblende grain (ultrasonically cleaned to remove clay) taken from a soil in Ashe County, North Carolina, U.S.A. Note prominent lens-shaped etch pits.

Table 1. Dissolution rate-controlling mechanism for various substances arranged in order of solubilities in pure water (mass of mineral which will dissolve to equilibrium.) (After Berner, 1978a; 1980)

Substance	Solubility mole per liter	Dissolution rate control
$Ca_5(PO_4)_3OH$	2×10^{-8}	Surface-reaction
$KAlSi_3O_8$	3×10^{-7}	Surface-reaction
$NaAlSi_3O_8$	6×10^{-7}	Surface-reaction
$BaSO_4$	1×10^{-5}	Surface-reaction
AgCl	1×10^{-5}	Transport
$SrCO_3$	3×10^{-5}	Surface-reaction
$CaCO_3$	6×10^{-5}	Surface-reaction
Ag_2CrO_4	1×10^{-4}	Surface-reaction
$PbSO_4$	1×10^{-4}	Mixed
$Ba(IO_3)_2$	8×10^{-4}	Transport
$SrSO_4$	9×10^{-4}	Surface-reaction
Opaline SiO_2	2×10^{-3}	Surface-reaction
$CaSO_4 \cdot 2H_2O$	5×10^{-3}	Transport
$Na_2SO_4 \cdot 10H_2O$	2×10^{-1}	Transport
$MgSO_4 \cdot 7H_2O$	3×10^{0}	Transport
$Na_2CO_3 \cdot 10H_2O$	3×10^{0}	Transport
KCl	4×10^{0}	Transport
NaCl	5×10^{0}	Transport
$MgCl_2 \cdot 6H_2O$	5×10^{0}	Transport

A simple calculation shows how incorrect it is to assume that a typical, relatively insoluble, mineral dissolves during weathering at a rate predicted for diffusion or transport control in aqueous solution. Using the solubility for K-feldspar at a soil pH of 6 (rather than the value given in Table 1 which is for a hydrolysis pH of 8), typical values of $D_s = 10^{-6}$ $cm^2 sec^{-1}$ and $r_c = 200$ μm, and the reasonable assumption for dilute soil solutions that $C_\infty << C_{eq}$, we obtain from equation (2) the time necessary to completely dissolve 200 μm sized feldspar grains by molecular diffusion in solution. The result is t = 14 months. (This is a maximum value since flow of the soil or ground water has not been considered.) Obviously, this result is incorrect since K-feldspars persist in soils for thousands to millions

of years; thus, actual dissolution rate is far slower than that predicted for aqueous diffusion control.

DIAGENESIS

Diagenesis, especially early diagenesis, lends itself readily to a kinetic approach. The principal reason for this is that a time frame is associated with sedimentary layers. In modern unlithified sediments overlain by water, the most convenient frame of reference is the sediment-water interface. Depth below this interface is proportional to time, and burial can be viewed as the flow of sediment downward away from the interface. If one, then, fixes on a given depth in a sediment, processes affecting chemical properties at that depth must also include burial advection. Also, since vertical concentration gradients are generally much greater than horizontal ones, one can treat the properties as being only a function of depth and time. Mathematically, these ideas can be expressed in the form of a diagenetic equation:

$$\left(\frac{\partial C}{\partial t}\right)_x = \frac{dC}{dt} - \omega\left(\frac{\partial C}{\partial x}\right)_t \qquad (4)$$

where: C = concentration, x = depth in the sediment, t = time, and ω = rate of burial (dx/dt). Here the partial derivative refers to changes at any fixed depth x and the total derivative refers to changes occurring in a fixed sediment layer undergoing burial.

A very useful concept is that of steady state diagenesis. This occurs when all diagenetic processes balance one another so that there is no change with time at a given depth. Mathematically, this is expressed as:

$$\left(\frac{\partial C}{\partial t}\right)_x = 0 \qquad (5)$$

so that from (4):

$$\frac{dC}{dt} = \omega\left(\frac{\partial C}{\partial x}\right)_t \qquad (6)$$

Steady state diagenesis can be viewed as a balance set up such that material supplied or depleted from above by burial is consumed or produced by chemical reaction (and diffusion) and, as a result, plots of concentration versus depth always look the same at successive times. This is all illustrated in Figure 9. Note that there is diagenetic

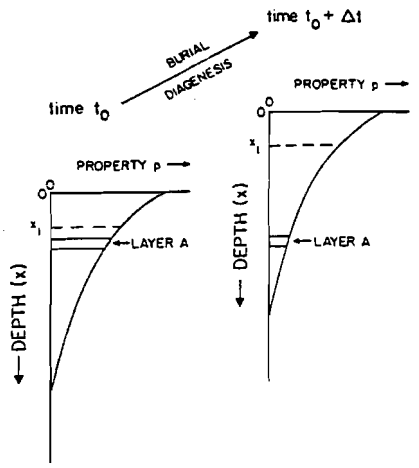

Figure 9. Diagramatic representation of steady state diagenesis. Upon burial, the value of property p does not change for a fixed depth x_1 (or $x = 0$), but does change for a fixed layer A. (After Berner, 1980)

change within a given layer undergoing burial but no change at a fixed depth. Since the sediment-water interface is also a fixed depth ($x = 0$), steady state diagenesis means that the composition of material added to the sediment at the time of deposition does not vary with time. Obviously, steady state is most likely where depositional conditions are constant and continuous. This is best exhibited by fine-grained muds deposited in lakes or the oceans.

The treatment of diagenesis in this paper will be restricted to a brief discussion of organic matter decomposition, via sulfate reduction, in fine-grained marine sediments. This is done merely to demonstrate a chemical kinetic approach to diagenesis and is not intended as a thorough treatment of either bacterial sulfate reduction or diagenetic processes. For a more complete discussion of quantitative approaches to diagenesis, the reader is referred to the book by Berner (1980). Here we will ignore the processes of compaction, bioturbation, adsorption, and externally forced water flow, and will concentrate only on chemical reaction, burial advection, and interstitial molecular diffusion. Also, only steady state diagenesis will be considered. In the case of sulfate reduction these assumptions are reasonably valid if we restrict our discussion to sediment depths below the top 10-20 cm where bioturbation (the disturbance of bottom sediment by macroorganisms) and consequent water movement can be appreciable. Also, sulfate does not strongly adsorb on solid particles in most sediments.

Bacterial sulfate reduction involves the reduction of dissolved sulfate in the interstitial water of a sediment to H_2S with a concomitant oxidation of organic matter to CO_2 and HCO_3^-. The overall process can be summarized by the reaction:

$$2CH_2O + SO_4^{2-} \rightarrow H_2S + 2HCO_3^- \qquad (7)$$

This process can take place only under strictly anoxic conditions and as a result it is normally restricted to buried sediments since most all surface waters contain dissolved oxygen. Sulfate reduction is an important process both for the decomposition of organic matter and for the formation of pyrite (which forms by the reaction of H_2S with detrital iron minerals in the sediment).

The rate of organic matter decomposition via sulfate reduction can be assumed to follow first-order kinetics as discussed earlier in this paper (see also Chapter 1). In other words, in terms of equation (3):

$$\frac{dG}{dt} = -kG \tag{8}$$

where G now refers to the concentration of CH_2O in reaction (7). (For reasons that will soon become apparent, G is expressed in units of mass of solid organic carbon per unit volume of enclosing pore water.) If we assume that the organic matter is present in a solid form so that the only processes affecting it are burial advection and decomposition, and that it consists of only one set of organic compounds with one k value (which is reasonable for sediments below the zone of bioturbation), then from equations (6) and (8) at steady state:

$$-\omega \frac{\partial G}{\partial x} - kG = 0 \tag{9}$$

Solution of this equation for the boundary conditions;

$$\begin{array}{ll} x = 0 & x \to \infty \\ G = G_o & G \to 0 \end{array}$$

yields:

$$G = G_o \exp[-\frac{k}{\omega} x] \tag{10}$$

Now from the stoichiometry of reaction (7), the rate of bacterial sulfate reduction is given by:

$$\frac{dC}{dt}_{bact} = \frac{1}{2} \frac{dG}{dt} \tag{11}$$

where C = concentration of dissolved sulfate in mass per unit volume of interstitial water. (Equation (11) is simple since we have expressed G in terms of mass per unit volume of pore water.) From (8), (10), and (11), finally:

$$\frac{dC}{dt}_{bact} = -\frac{kG_o}{2} \exp[-\frac{k}{\omega} x] \tag{12}$$

The diagenetic equation for sulfate, since it is a dissolved species, involves diffusion as well as bacterial reduction and burial. At steady state the diagenetic equation is:

$$D_s \frac{\partial^2 C}{\partial x^2} - \omega \frac{\partial C}{\partial x} - \frac{kG_o}{2} \exp\left[-\frac{k}{\omega} x\right] = 0 \qquad (13)$$

where D_s = molecular diffusion coefficient of sulfate in the sediment. The first term on the left assumes that Fick's Second Law of diffusion describes the effect of diffusion on sulfate concentration. Solution of equation (13) for the boundary conditions:

$$\begin{array}{ll} x = 0 & x \to \infty \\ C = C_o & C \to C_\infty \end{array}$$

yields:

$$C = (C_o - C_\infty) \exp\left(-\frac{k}{\omega} x\right) + C_\infty \qquad (14)$$

$$C_o - C_\infty = \frac{\omega^2 G_o}{2(\omega^2 + kD_s)} \qquad (15)$$

(The asymptotic concentration C_∞ strictly represents the concentration of sulfate when organic matter is exhausted, in other words, when G goes to zero. However, in most sediments sulfate is exhausted before organic matter and in this case C_∞ becomes a negative number and is used only as a curve fit parameter.)

From plots of measured dissolved sulfate concentrations versus depth, such as that shown in Figure 10, the values of k and G_o can be obtained by a combination of curve fitting to obtain C_o, C_∞, and k/ω and the use of independently determined values of ω and D_s. This has been done for a wide variety of sediments (Toth and Lerman, 1977; Berner, 1978b; 1980; Murray *et al.*, 1978; Filipek and Owen, 1980) resulting in values of k ranging over six orders of magnitude. Values of G_o are much more uniform. In this way, use of diagenetic equations along with sediment chemical data can be used to obtain fundamental rate data for organic matter decomposition.

The model presented above assumes that the rate of sulfate reduction is a function only of the concentration of metabolizable organic carbon and not also of sulfate. From a number of laboratory studies using natural sediments (*e.g.*, Martens and Berner, 1977) this is justified but only at sulfate concentrations greater than about 25% of that

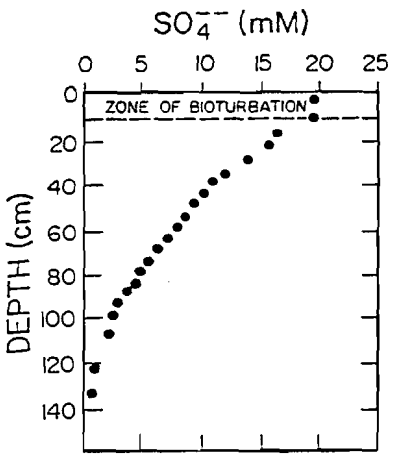

Figure 10. Representative sulfate concentration profile from an organic-rich nearshore sediment (FOAM site) from Long Island Sound, N.Y., U.S.A (Modified after Goldhaber, 1977)

found in the overlying seawater. As sulfate is depleted with depth to very low values, the rate of sulfate reduction in most sediments must become limited by sulfate itself. Recent unpublished laboratory experiments by Joseph Westrich at Yale University shows this to be the case. Westrich has found that in order to describe bacterial sulfate reduction at all depths and all sulfate concentrations, equation (12) must be modified to:

$$\left(\frac{dC}{dt}\right)_{bact} = -\frac{kG_o}{2}\exp\left[-\frac{k}{\omega}x\right]\left(\frac{C}{K_M+C}\right) \quad (16)$$

where K_M = curve fit parameter with the units of concentration. This dependence upon sulfate concentration shows that sulfate reduction obeys the Michaelis-Menten equation (Cornish-Bowden, 1976) which is a common rate law for bacterial processes. In this case K_M is referred to as the Michaelis constant. For sediments buried well below the zone of bioturbation Westrich found the value of K_M to average around 1.5 mM. Thus, at most sulfate concentrations, such as shown in Figure 10, equation (16) is sufficiently accurately represented by the much more simple equation (12) and the type of diagenetic modeling discussed above is justified. Use of equation (16), instead of (12), in the diagenetic equation would lead to a more complicated solution since in this case the diagenetic equation becomes non-linear.

CONCLUSION

In this paper I have tried to show how the subjects of weathering and diagenesis can be approached from a kinetic standpoint. This type of work depends upon an intimate interplay between field measurements, laboratory experiments, and mathematical theory. Because of the accessibility of soils and sediments, models based on laboratory measurements and theoretical calculations can be used along with field data to

calculate rate parameters which are otherwise difficult to measure in the laboratory. Also, theoretical models can be tested in the field. Much more work needs to be done in the application of chemical kinetics to geological problems, and it is hoped that this chapter has shown some of the ways this can be done for the surficial environment.

ACKNOWLEDGMENTS

Research was supported by National Science Foundation Grants EAR 80-07815 and OCE 79-06919.

CHAPTER 3 REFERENCES

Aagaard, P. and Helgeson, H. C. (1981) Thermodynamic and kinetic constraints on reaction rates among minerals and aqueous solutions. I. Theoretical considerations. Amer. J. Sci. (in press).

Berner, R. A. (1974) Kinetic models for the early diagenesis of nitrogen, sulfur, phosphorus, and silicon in anoxic marine sediments. In E. D. Goldberg (ed.), *The Sea*, vol. 5, Wiley, New York, p. 427-450.

_____ (1978a) Rate control of mineral dissolution under earth surface conditions. Amer. J. Sci., 278, 1235-1252.

_____ (1978b) Sulfate reduction and the rate of deposition of marine sediments. Earth Planet. Sci. Letters, 37, 492-498.

_____ (1980) *Early Diagenesis: A Theoretical Approach*. Princeton Univ. Press, Princeton, New Jersey, 241 p.

_____ and Holdren, G. R., Jr. (1979) Mechanism of feldspar weathering -- II. Observations of feldspars from soils. Geochim. Cosmochim. Acta, 43, 1173-1186.

_____ and Morse, J. W. (1974) Dissolution kinetics of calcium carbonate in seawater: IV. Theory of calcite dissolution. Amer. J. Sci., 274, 108-134.

_____, Sjöberg, E. L., Velbel, M. A., and Krom, M. D. (1980) Dissolution of pyroxenes and amphiboles during weathering. Science, 207, 1205-1206.

Burton, W. K., Cabrera, N., and Frank, F. C. (1951) The growth of crystals and the equilibrium structure of their surfaces. Royal Soc. London Philos. Trans., A-243, 299-358.

Busenberg, E. and Clemency, C. V. (1976) The dissolution kinetics of feldspars at 25°C and 1 atm CO_2 partial pressure. Geochim. Cosmochim. Acta, 40, 41-50.

Claypool, G. and Kaplan, I. R. (1974) The origin and distribution of methane in marine sediments. In I. R. Kaplan (ed.), *Natural Gases in Marine Sediments*, Plenum, New York, p. 99-139.

Cornish-Bowden, A. (1976) *Principles of Enzyme Kinetics*, Butterworths, London, 206 p.

Dibble, W. E., Jr. and Tiller, W. A. (1981) Non-equilibrium water/rock interactions -- I. Model for interface-controlled reactions. Geochim. Cosmochim. Acta, 45, 79-92.

Filipek, L. H. and Owen, R. M. (1980) Early diagenesis of organic carbon and sulfur in outer shelf sediments from the Gulf of Mexico. Amer. J. Sci., 280, 1097-1112.

Fouillac, C., Michard, G., and Bocquier, G. (1977) Une méthode de simulation de l'évolution des profils d'altération. Geochim. Cosmochim. Acta, 41, 207-213.

Fritz, B. (1975) Étude thermodynamique et simulation des réactions entre mineraux et solutions. Application a la géochimie des altérations et des eaux continentales. Univ. Louis Pasteur de Strasbourg, Inst. de Geologie, Mem. 41, 153 p.

Gac, J. Y., Badaut, D., Al-Droubi, A. and Tardy, Y. (1978) Compartement du calcium du magnésium et de la silice en solution. Précipitation de calcite magnésienne, de silice amorphe, et de silicates magnésiens au cors de l'evaporation des eaux du Chari (Tchad). Sci. Géol. Bull. (France), 31, 185-193.

Goldhaber, M. B., Aller, R. C., Cochran, J. K., Rosenfeld, J. K., Martens, C. S. and Berner, R. A. (1977) Sulfate reduction, diffusion, and bioturbation in Long Island Sound sediments: Report of the FOAM group. Amer. J. Sci., 277, 193-237.

Helgeson, H. C. (1971) Kinetics of mass transfer among silicates and aqueous solutions. Geochim. Cosmochim. Acta, 35, 421-469.

_____, Garrels, R. M., and MacKenzie, F. T. (1969) Evaluation of irreversible reactions in geochemical processes involving minerals and aqueous solutions -- II. Application. Geochim. Cosmochim. Acta, 33, 455-481.

Holdren, G. R., Jr. and Berner, R. A. (1979) Mechanism of feldspar weathering -- I. Experimental studies. Geochim. Cosmochim. Acta, 43, 1161-1171.

Jørgensen, B. B. (1978) Comparison of methods for the quantification of bacterial sulfate reduction in coastal marine sediments. II. Calculation from mathematical models. Geomicrobiology J., 1, 20-47.

Keir, R. S. (1980) The dissolution kinetics of biogenic calcium carbonates in seawater. Geochim. Cosmochim. Acta, 44, 241-252.

Keith, R. E. and Gilman, J. J. (1960) Dislocation etch pits and plastic deformation in calcite. Acta Metall., 8, 1-10.

Lindsay, W. (1979) *Chemical Equilibria in Soils*. John Wiley, New York, 449 p.

Martens, C. S. and Berner, R. A. (1977) Interstitial water chemistry of anoxic Long Island Sound sediments. I. Dissolved gases. Limnology and Oceanography, 22, 10-25.

Morse, J. W. (1978) Dissolution kinetics of calcium carbonate in sea water: VI. The near equilibrium dissolution kinetics of calcium carbonate-rich deep sea sediments. Amer. J. Sci., 278, 344-353.

_____ and Berner, R. A. (1979) The chemistry of calcium carbonate in the deep oceans. In E. A. Jenne (ed.), *Chemical Modeling--Speciation, Sorption, Solubility and Kinetics in Aqueous Systems*. Amer. Chem. Soc. Symposium Series, No. 93, 499-535.

Murray, J. W., Grundmanis, V. and Smethie, W. M. (1978) Interstitial water chemistry in the sediments of Saanich Inlet. Geochim. Cosmochim. Acta, 42, 1011-1026.

Nielsen, A. E. (1964) *Kinetics of Precipitation*. MacMillan, New York, 151 p.

_____ and Sõhnel, O. (1971) Interfacial tensions electrolyte crystal-aqueous solution from nucleation data. Jr. Crystal Growth, 11, 233-242.

Ohara, M. and Reid, R. C. (1973) *Modeling Crystal Growth Rates from Solution*. Prentice-Hall, Englewood Cliffs, New Jersey, 272 p.

Pačes, T. (1973) Steady state kinetics and equilibrium between ground water and granitic rock. Geochim. Cosmochim. Acta, 37, 2641-2663.

Petrović, R. (1976) Rate control in feldspar dissolution -- II. The protective effect of precipitates. Geochim. Cosmochim. Acta, 40, 1509-1522.

_____, Berner, R. A., and Goldhaber, M. B. (1976) Rate control in dissolution of alkali feldspars — I. Study of residual feldspar grains by X-ray photoelectron spectroscopy. Geochim. Cosmochim. Acta, 40, 537-548.

Schott, J., Berner, R. A., and Sjöberg, E. L. (1981) Mechanism of pyroxene and amphibole weathering. I. Experimental studies of iron-free minerals. (Submitted to Geochim. Cosmochim. Acta.)

Tardy, Y., Cheverry, C., and Fritz, B. (1974) Neoformation d'une argile magnésienne dans les dépressions interdunaires du lac Tchad. Application aux domaines de stabilité des phyllosilicates alumineux, magnésiens, et ferrifères. C. R. Acad. Sci., Paris, Ser. D., 278, 1999-2002.

Toth, D. J. and Lerman, A. (1977) Organic matter reactivity and sedimentation rates in the ocean. Amer. J. Sci., 277, 265-285.

Wilson, M. J.,(1975) Chemical weathering of some primary rock-forming minerals. Soil Sci., 119, 349-355.

Chapter 4

TRANSITION STATE THEORY

Antonio C. Lasaga

INTRODUCTION

Most kinetic phenomena from the microscopic viewpoint consist of a sequence of elementary steps, each of which requires overcoming a potential energy barrier. The microscopic dynamics may be likened to a geologist who travels from valley to valley by climbing over successive ridges and hopefully finds the easiest mountain passes between potential energy peaks. The task of transition state theory (TST) is to characterize precisely the climbing rates of reactants over these potential barriers. This powerful theory dates back to a series of papers in 1935 by Henry Eyring (Eyring, 1935a,b; Glasstone *et al.*, 1941) who developed a statistical mechanical calculation of reaction velocities. We can explain the tenets of the theory as follows. An *elementary* reaction involves the molecular collision of reactant species to produce specified products. Both reactants and products are situated at the bottom of well-defined potential energy wells; i.e., they are stable (or metastable) species. However, in proceeding from reactants to products, the species must usually travel over a potential energy barrier (see Fig. 1a). The theory at this point focuses on the molecular configuration at the top of this barrier, (ABC)*, a configuration roughly midway between that of reactants and products. The potential energy surface has a maximum at this configuration in the direction of the so-called *reaction coordinate*, but the potential energy increases in all other directions. Therefore, the potential energy surface topology in the neighborhood of this configuration, termed the *activated complex*, resembles that of a saddle. The reaction coordinate (dashed line in Fig. 1a) is the net motion which takes reactants to products. For example, for the reaction $A + BC \rightarrow AB + C$, motion along the reaction coordinate (see Fig. 1a) alters the configuration of the atoms as follows:

$$\vec{A} - - - \vec{B} - - - \vec{C} . \qquad (1)$$

This motion illustrates the decrease in the r_{AB} distance and the concomitant increase in the r_{BC} distance needed to form the products.